

ABSTRACT

With their ability to adhere to a wide variety of underwater surfaces, mussels have inspired a new line of investigation into surface chemistry and adhesives. This unique ability is due to byssal threads that mussels excrete, composed of proteins with a high concentration of the amino acid 3,4-dihydroxyphenylalanine (DOPA). Dopamine (DA), a small molecule mimic of DOPA, is able to polymerize under oxidizing conditions. Polydopamine (PDA) is known as a universal adhesive, although its adhesive properties are affected by many different experimental variables, including pH, buffer type, oxidizing agent, substrate, and coating method. Previous research in the Chen lab has determined the optimized conditions for spin coating PDA. These include DA concentration of 4 mg/mL, sodium periodate (SP) as the oxidizing agent with [SP]:[DA] = 2, 0.25 M pH = 6 acetate buffer, and 1 min adhesion time prior to spin.

This project focuses on the differences in PDA adhesion on substrates with varying functional groups. PDA is able to form many different chemical interactions, but it is limited by the chemistry of the substrate. This project examines PDA adhesion on native silicon wafers (SiO₂) and substrates containing polydimethylsiloxane (PDMS) and aminopropyl methylsiloxane – dimethylsiloxane copolymer (PADMS). PDMS and PADMS are chemically similar; however, continuous PDA morphology is obtained on SiO₂ and PADMS, while the PDA films contain cracks on PDMS. When PDMS and PADMS polymers were mixed to form composite substrates, only a minuscule fraction of PADMS, 1/20,000, is required for the morphology of the adhered PDA film to utilize the same growth mechanism as that on pure PADMS. In order to form a continuous film on pure PDMS, the buffer solution was diluted to reduce interference from salt ions.

Dip coating is the traditional method of PDA film deposition; however, the research for this project was conducted using spin coating. Therefore, a modified dip coating method was created in order to ensure that any conclusions drawn from this research would be relevant for both spin and dip coating. Additionally, in an attempt to extend the lifespan of PDA solutions, the pH was lowered at the aging time with the most adhesive particles in solution. This would theoretically halt additional polymerization and allow one PDA solution to be used multiple times.

CONTINUITY AND GROWTH MECHANISM OF POLYDOPAMINE THIN FILMS

Katherine Kolozsvari

**A thesis presented to the faculty of Mount Holyoke College in
partial fulfillment of the requirements for the degree of
Bachelor of Arts with Honors**

Department of Chemistry

South Hadley, Massachusetts

May 2021

This thesis was prepared under the direction of Dr. Wei Chen
for 8 credits of independent study

ACKNOWLEDGEMENTS

I am incredibly honored by all of the support that I have received through this process. Especially completing this during a pandemic, I have been blown away by all of the virtual support that I have gotten, and I will forever be thankful to everyone who has helped me in both large and small ways.

First, I am honored to thank Professor Wei Chen for her unending support over the last four years. Since my first year on campus, she has been an amazing mentor and I cannot imagine my Mount Holyoke experience without her. She helped me to discover my love of both chemistry and research, and she has always been there to guide and help me through everything. She has gifted me with endless support and wisdom, and I have been incredibly lucky to have her as a P.I., professor, and mentor.

I'm also incredibly grateful to both Professor Katie McMenimen and Professor Amanda Maciuba for serving on my thesis committee. Especially with so much going on in the world this year, I am beyond thankful to them for all their help.

I would also like to thank Professor Himali Jayathilake for her thoughtful insights during group meeting and for her unending support and kindness she's shown me since I've met her.

My incredible peers in the lab have never failed to make my days brighter. I would like to thank Jiuk Byun for her mentorship, Maggie Minett, Yuxin Jiang, Anya Chinniah, Liz Hazen, Wenyun Wang, Carolina Alvarez, Carlie Poworoznek, Julia Griffin, and Nancy Jiang for their friendship, support, and fantastic ideas.

I would be remiss not to include the Mount Holyoke Swim and Dive team in the list of people who have supported me through this process. My coaches, Rachael Araujo and Dave Allen as well as all my teammates have become my second family and support system on campus. I'm so grateful to have met them and for all the time we've spent together. An especially huge thank you to Ashton Bliss, Sam Nemivant, Natalie Burkett, Adrienne Corr, and Kathryn Murphy who helped me make sure my research presentations were

accessible to a wide audience and who were willing to be my lab buddy when I needed a second person for late night after practice lab work.

Finally, I am incredibly grateful for my parents and siblings for their unconditional love and support both through this thesis and for my entire life. I would not be able to do any of the things that I've done without them and I don't know how I got so incredibly lucky to have such an amazing family. Especially in the fall when I was attending Mount Holyoke virtually from home, my family supported me unendingly, and were always willing to lend an ear or a hug when I needed it.

TABLE OF CONTENTS

	Page Number
ACKNOWLEDGMENTS	i
TABLE OF CONTENTS	iii
LIST OF FIGURES AND TABLES	vi
CHAPTER I. INTRODUCTION	1
1.1 Mussel-Inspired Surface Chemistry	1
1.1.1 Mussel Foot Protein Adhesion	1
1.1.2 DOPA and Catecholamine Chemistry	3
1.2 Dopamine	6
1.2.1 Applications	7
1.3 Polymerization of Dopamine	8
1.3.1 Proposed Mechanisms	8
1.3.2 Polymerization Factors	11
1.4 Coating Methods	13
1.4.1 Dip Coating	13
1.4.2 Spray Coating	14
1.4.3 Spin Coating	15
1.5 Substrate Chemistry	16
1.6 Project Overview	19

CHAPTER II. MATERIALS AND METHODS	21
2.1 Materials	21
2.2 Preparation of DA Solutions	22
2.3 Substrate Preparation	22
2.3.1 SiO ₂	22
2.3.2 PDMS and PADMS	23
2.3.3 PDMS-PADMS Mixtures	23
2.4 Coating Methods	23
2.4.1 Spin Coating	23
2.4.2 Modified Dip Coating	24
2.5 Characterization Methods	25
2.5.1 Thickness	25
2.5.2 Contact Angle	25
2.5.3 Atomic Force Microscopy	25
2.5.4 Optical Microscopy	26
CHAPTER III: RESULTS AND DISCUSSION	27
3.1 Substrate Chemistry	27
3.2 Spin Coating PDA at Various Aging Times	28
3.2.1 Thickness and Contact Angle	28
3.2.2 Optical Microscopy	31
3.2.3 Atomic Force Microscopy	33

3.3 Spin Coating PDA on Substrates Containing PADMS and PDMS Mixtures	35
3.3.1 Thickness	35
3.3.2 Atomic Force Microscopy and Contact Angle	36
3.4 Buffer Dilution	39
3.4.1 Thickness	39
3.4.2 Atomic Force Microscopy and Contact Angle	40
3.5 Modified Dip Coating	42
3.5.1 Thickness and Contact Angle	42
3.5.2 Atomic Force Microscopy	45
3.6 “Freezing” PDA	47
CHAPTER IV: CONCLUSIONS & FUTURE WORK	49
REFERENCES CITED	54

LIST OF FIGURES AND TABLES

	Page Number
Figure 1. A diagram of a byssal plaque, demonstrating the relative positions of the major mfps. Mfp-3 and mfp-5 are integral to surface adhesion, while mfp-6 helps to maintain the chemical environment necessary for adhesion (A). Pie charts illustrating the amino acid compositions of key mfps (B). ³	3
Figure 2. Representation of four types of chemical interactions between catechols and substrates: hydrogen bonding (A), π - π stacking (B), coordination with metallic surfaces (C), and covalent bonding to an amine (D).	4
Figure 3. Rescue paths of dopaquinone back into adhesive forms.	6
Figure 4. Chemical structures of dopamine and L-DOPA.	7
Figure 5. Schematic of PDA use as a primer, with the 2 ^o coating tailored to an application. ⁵	8
Figure 6. Auto-oxidation of a generic catechol to a quinone in the presence of oxygen. ¹³	9
Figure 7. Current understanding of the polymerization mechanism for PDA.	10
Figure 8. Original dip coating method used by Lee et al. ¹	14
Figure 9. Spray coating method, as used by Hong et al. ³¹	15
Figure 10. Schematic of the four steps of spin coating.	16
Figure 11. Chemical structures of the three substrates used in this experiment. The two polymer substrates were covalently adhered to a silicon wafer base.	17

Figure 12. PDMS compared with its carbon backbone counterpart. Bond lengths are shown in pink, bond angles are shown in blue, electronegativity and percent ionic character are shown in red. ³⁹	18
Figure 13. Thickness of PDA on all substrates. Time indicates the aging time of the DA solution from the point when dopamine hydrochloride was added until the solution was introduced to the substrate. For all samples, the DA solution was in contact with the substrate for 1 min before spin.	29
Figure 14. Advancing and receding dynamic contact angles of PDA on PADMS and SiO ₂ . The 0 time point indicates the contact angles of the substrates with no PDA.	30
Figure 15. Advancing and receding dynamic contact angles of PDA on PDMS. The 0 time point indicates the contact angles of unmodified PDMS.	30
Figure 16. Thickness of PDA on substrates containing polymer mixtures as a function of fraction of PADMS in polymer mixture.	36
Figure 17. Advancing and receding dynamic contact angles of PDA spin cast after 1 min aging time on substrates containing polymer mixtures.	38
Figure 18. Advancing and receding dynamic contact angles of substrates containing polymer mixtures.	38
Figure 19. Thickness of PDA on PDMS as a function of aging time, using a 5x diluted buffer solution.	40
Figure 20. Advancing and receding dynamic contact angles of PDA on PDMS using a 5x diluted buffer solution.	42
Figure 21. Thickness of PDA on SiO ₂ using both modified dip and spin coating as a function of PDA aging time.	44
Figure 22. Dynamic contact angles of PDA on SiO ₂ using modified dip and spin coating as a function of PDA aging time.	45

Figure 23. Thickness of PDA on PADMS as a function of time after HCl was added to the PDA solution.	48
Table 1. Images of PDA solutions at different aging times using various oxidants, pHs, and buffers. ²⁵	12
Table 2. Substrates and their interactions with PDA. ¹⁸	17
Table 3. Substrate thickness and contact angle.	28
Table 4. Optical images at 10x magnification of PDA on all substrates as a function of PDA aging time, with a scale bar of 200 μm .	32
Table 5. AFM images (size: 1.25 x 5 μm^2 , height scale: 20 nm) of PDA on all substrates as a function of PDA aging time.	34
Table 6. AFM images (size: 1.25 x 5 μm^2 , height scale: 20 nm) of PDA spin cast after 1 min aging time on polymer mixtures. The different polymer compositions are represented by the volume fraction of PADMS present.	37
Table 7. AFM images (size: 1.25 x 5 μm^2 , height scale: 20 nm) of PDA spin cast on PDMS using a 5x diluted buffer solution.	41
Table 8. AFM images (size 1.25 x 5 μm^2 , height scale: 20 nm) of PDA on SiO_2 using modified dip and spin coating.	46

I. INTRODUCTION

Since its introduction in 2007,¹ research on the adhesive properties of polydopamine (PDA) has branched into many different methods and objectives. The use of PDA as a surface modifier was inspired by the adhesive properties of mussels, whose byssal threads can strongly adhere to a wide range of surfaces underwater.¹ This ability is highly influenced by the chemical environment created by the amino acids present near the substrate. One amino acid important to adhesion is 3,4-dihydroxyphenylalanine (DOPA), which has a catecholamine structure. Dopamine, also a catecholamine, is a small molecule mimic of DOPA. It can self-polymerize into PDA in the presence of an oxidant, and it also has the ability to form many types of chemical interactions. This versatility allows PDA to be a universal adhesive, meaning that it can attach to almost any substrate. Despite this label of universal, the morphology, thickness, and chemical properties of PDA films depend on many experimental factors including nature of substrate, coating method, oxidant type, pH, and aging time.

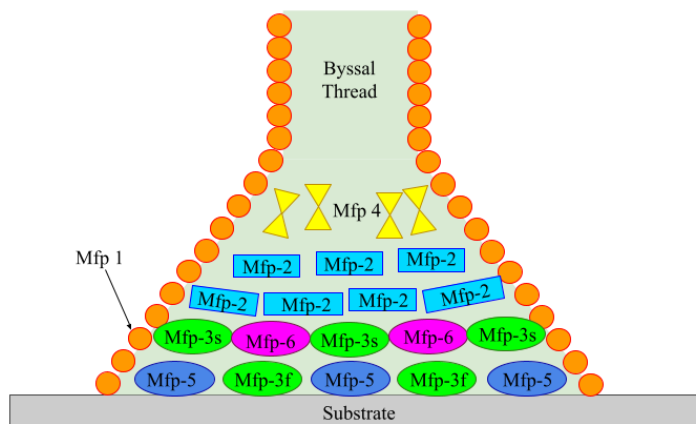
1.1 Mussel-Inspired Surface Chemistry

1.1.1 Mussel Foot Protein Adhesion

In order to strongly adhere to underwater surfaces, mussels expel byssal threads ending in adhesive plaques. These byssal plaques are composed of

several different proteins groups, called mussel foot proteins (mfps).² Each mfp is composed of a different mixture of amino acid residues to create a chemical environment that allows the mussel to adhere to a surface (Figure 1). Mfp-3f and mfp-5 are in direct contact with the substrate and are therefore the most directly involved in surface adhesion. Both of these proteins have a high concentration of DOPA (Figure 1),³ indicating that the DOPA functional group plays an important role in giving the plaques the ability to adhere to a substrate.

A.



B.

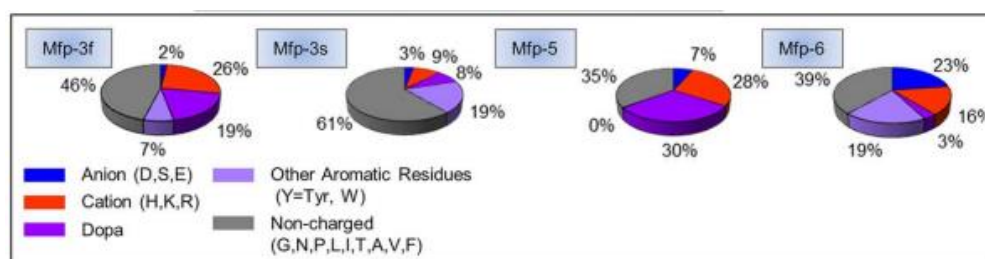


Figure 1. A diagram of a byssal plaque, demonstrating the relative positions of the major mfps. Mfp-3 and mfp-5 are integral to surface adhesion, while mfp-6 helps to maintain the chemical environment necessary for adhesion (A). Pie charts illustrating the amino acid compositions of key mfps (B).³

1.1.2 DOPA and Catecholamine Chemistry

DOPA is created through post-translational hydroxylation of tyrosine and is a very adhesive species due to its catechol and amine groups.⁴ The catechol group, composed of a phenyl with two adjacent alcohols, is able to adhere to a wide range of substrates, as it is capable of many different

interactions ranging in strength from hydrophobic interactions to covalent bonds (Figure 2).⁴ The amine group is able to participate in hydrogen bonding and covalent interactions. This versatility allows catecholamines, including DOPA, to adapt to the chemistry of a particular substrate. It is this property which causes catecholamines to be particularly useful as primers to alter the surface chemistry of many different substrates.^{1,5}

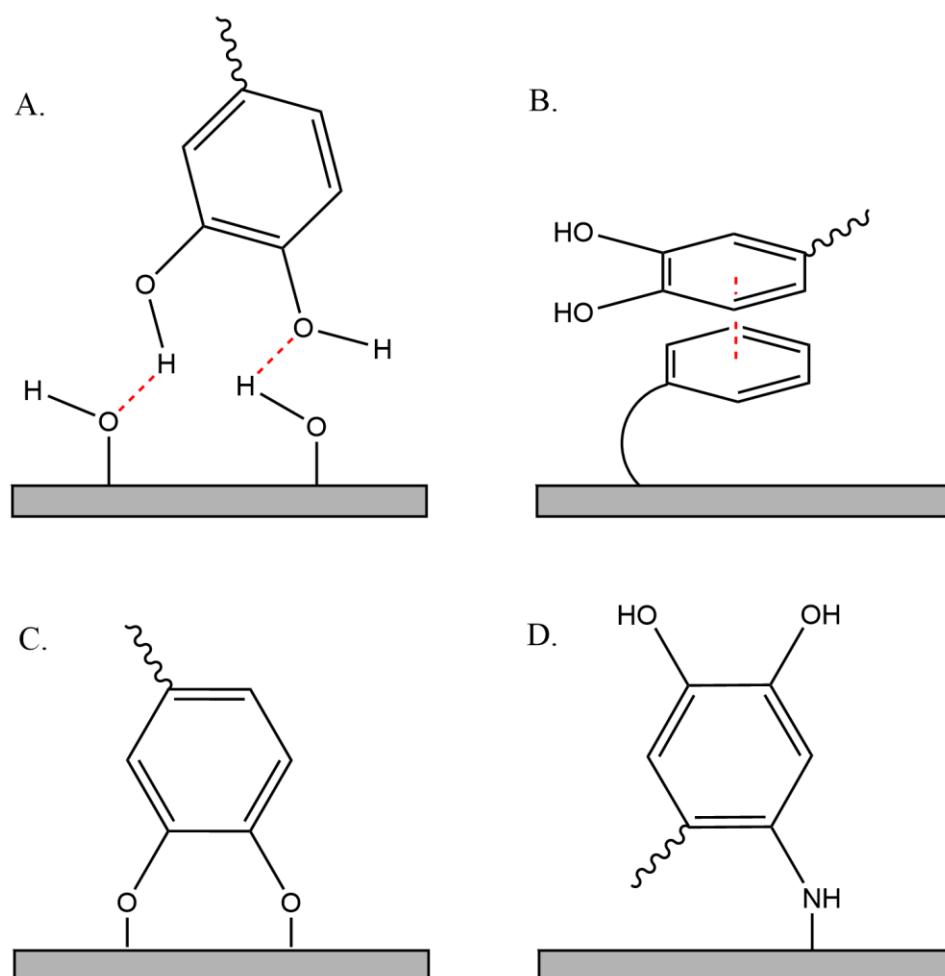


Figure 2. Representation of four types of chemical interactions between catechols and substrates: hydrogen bonding (A), π - π stacking (B), coordination with metallic surfaces (C), and covalent bonding to an amine (D).

DOPA alone is not solely responsible for the adhesive properties of byssal plaques, however. The chemical environment created by the surrounding proteins is far different from that of seawater. The combination of mfps in the byssal plaque creates an environment with an acidic pH, low ionic strength, and a reducing redox potential, which provides optimal conditions for the underwater adhesion of the plaque.⁶ One of the critical balances that the mussel must maintain is the adhesive and cohesive properties of the amino acid residues. In broad terms, cohesive species stick to each other, while adhesive species stick to a substrate.

In the presence of O_2 or Fe^{3+} , DOPA can be oxidized to dopaquinone, a cohesive species. Since the mfps are already covalently polymerized via the protein backbone, they have no use for additional cohesion and therefore need to keep DOPA in an adhesive form. The byssal thread has two pathways to “rescue” dopaquinone back to an adhesive form, tautomerization to dehydrodopa, or reduction by thiol (Figure 3).⁷ This thiol reduction is accomplished by cysteine residues present in mfp-6 (Figure 1).

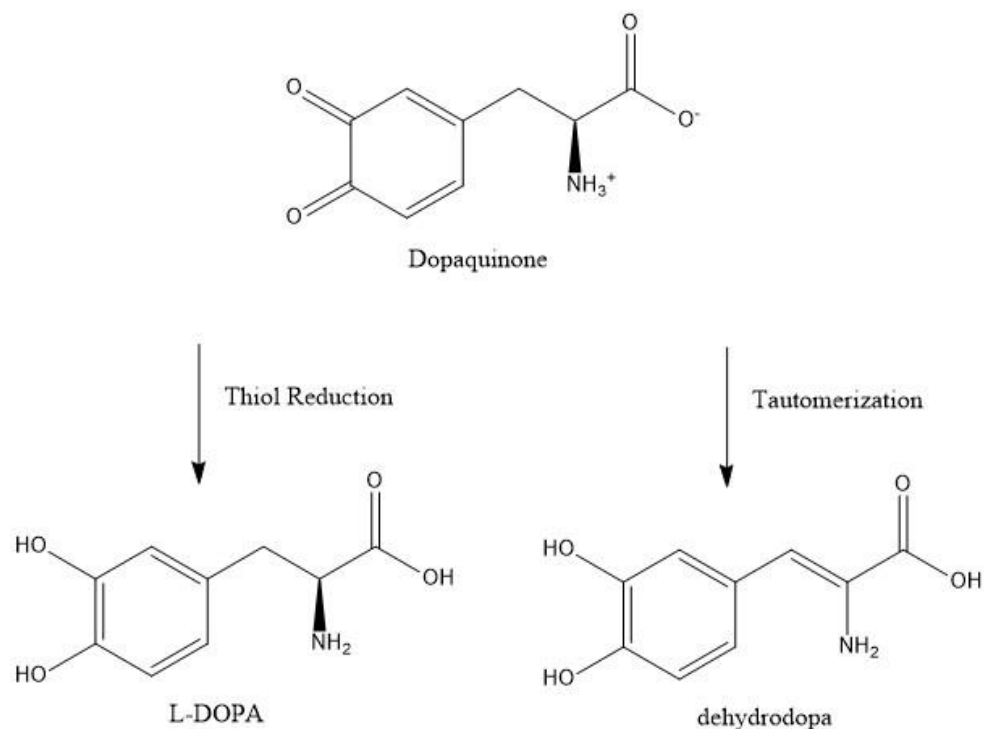


Figure 3. Rescue paths of dopaquinone back into adhesive forms.

1.2 Dopamine

Dopamine was identified as a small molecule mimic of DOPA due to its catecholamine structure,¹ which is very similar to that of DOPA (Figure 4). Once polymerized, PDA possesses universal adhesive properties similar to the byssal plaques it was inspired by, meaning that it can adhere to many substrates with different types of chemical properties.

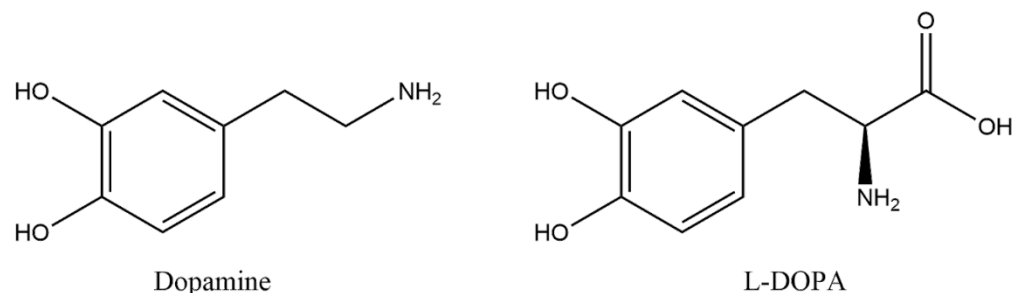


Figure 4. Chemical structures of dopamine and L-DOPA.

1.2.1 Applications

Due to its universal adhesive properties, polydopamine (PDA) has been investigated for a wide range of applications, including as a primer for secondary modifications,^{1,5,8} a biomedical adhesive,^{3,9} a coating for electronic devices,¹⁰ and as a drug delivery mechanism.^{11,12} Since PDA adhesion is a simple and efficient process, it can be useful in a wider variety of surface modifications compared to other coatings which require specific instrumentation or involve multi-step applications.¹ One of the most promising applications of PDA is that of a primer, as the secondary coating can be tailored to many different needs (Figure 5). This means that PDA has potential in a wide range of sectors including in industry, biomedicine, energy, and consumer.⁵

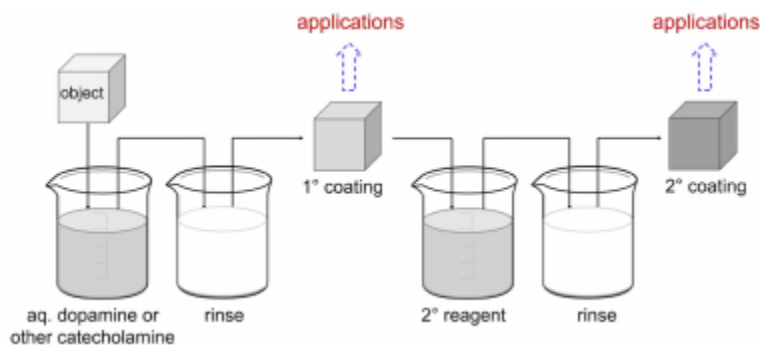


Figure 5. Schematic of PDA use as a primer, with the 2^o coating tailored to an application.⁵

1.3 Polymerization of Dopamine

1.3.1 Proposed Mechanisms

Due to the range of reactions dopamine can undergo, the exact mechanism of polymerization is not yet fully understood.¹³ However, it has been well documented that in the presence of oxygen, catechols, including dopamine, spontaneously oxidize to form a quinone through a semiquinone intermediate in a process called auto-oxidation (Figure 6).¹³⁻¹⁶ This reaction favors the reactants under a neutral pH; however, under alkaline conditions the equilibrium shifts towards polymerization due to the deprotonation of the hydroxyl groups on the catechol.¹³ Even under alkaline conditions, the kinetics of this reaction are slow due to the low solubility of oxygen in aqueous solutions¹⁷ and the low reduction potential of the reaction.¹³ This causes the

formation of PDA films using atmospheric oxygen as the oxidant to take hours to days to reach a useful thickness.^{1, 18}

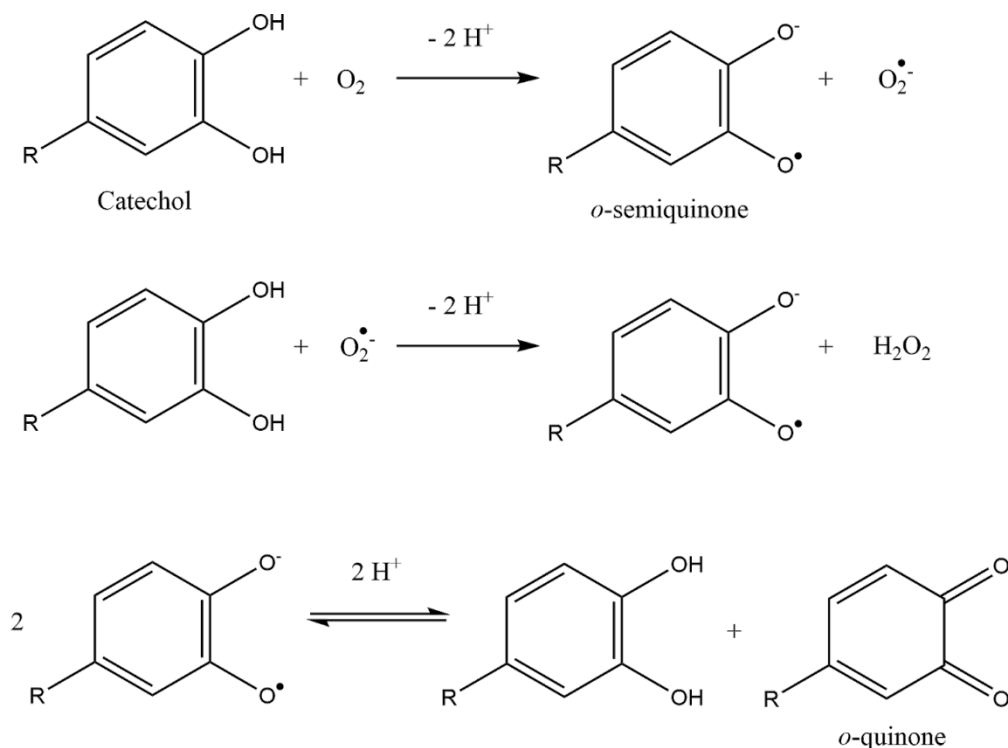


Figure 6. Auto-oxidation of a generic catechol to a quinone in the presence of oxygen.¹³

After oxidation to a quinone, dopamine can undergo cyclization and further oxidation to form dopaminechrome, which can then rearrange into 5,6-dihydroxyindole (DHI) (Figure 7).^{13,19} The exact mechanism of PDA formation has yet to be proved, however several proposed mechanisms involve both covalent and non-covalent interactions that aggregate in a structure analogous to eumelanin.²⁰⁻²² Although it has also been proposed that it is the differences

between eumelanin and PDA formation rather than the similarities that contributes to PDA adhesion.²³ It has been demonstrated that covalently bonded building blocks for PDA include DHI dimers as well as dopamine-DHI-DHI trimers, while (dopamine)₂/DHI complexes contribute to the non-covalent aggregation into PDA.²⁰ The unoxidized dopamine in these (dopamine)₂/DHI complexes do not appear to cause biological toxicity, as they are trapped within the structure of the PDA.²⁰

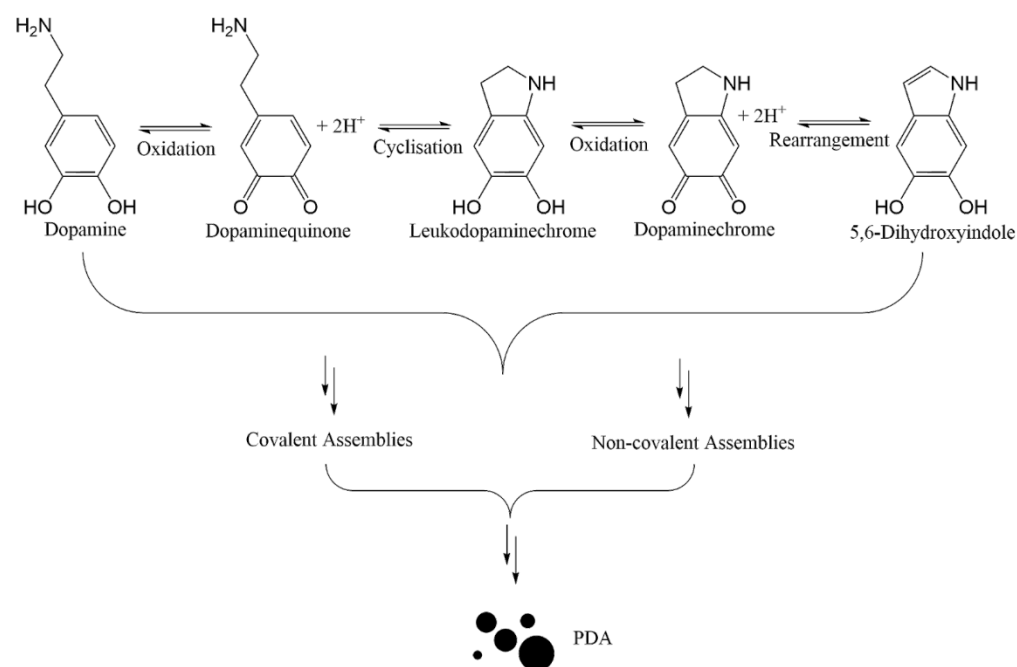





























Figure 7. Current understanding of the polymerization mechanism for PDA.

1.3.2 Polymerization Factors

In addition to the complexity of the mechanism of PDA formation, there are several factors which can alter the kinetics or structure of PDA, including the choice of pH, buffer, and oxidant. An example of how different conditions of polymerization can visually alter the solution is shown in Table 1, which compares polymerization using two oxidants: sodium periodate (SP) and O₂, as well as both carbonate and acetate buffers at varying pHs. As previously discussed, since the first step of polymerization is oxidation, increasing the pH shifts the equilibrium towards polymerization. This also has the effect of speeding up the formation of PDA under more alkaline conditions.¹⁸ The choice of buffer is also essential to the polymerization process and can affect the size and adhesive properties of PDA.²⁴ Tris buffer, which was used in the initial PDA study by Lee et al.¹ can be incorporated into the structure of polydopamine, inhibiting the cyclization of dopaminequinone and causing a slower polymerization compared to phosphate or carbonate buffers.²¹

Table 1. Images of PDA solutions at different aging times using various oxidants, pHs, and buffers.²⁵

	<1 min	1 min	2 min	4 min	30 min	1 hr	4 hr	10.5 hr
O ₂ pH: 8.5 Carbonate								
SP pH: 3.4 Acetate								
SP pH: 4.9 Acetate								
SP pH: 5.9 Acetate								

Since utilizing atmospheric oxygen as the oxidant has relatively slow reaction kinetics, chemical oxidants have been utilized to speed up the process of polymerization.^{18,26-28} Common chemical oxidants include SP, copper

sulfate, and ammonium persulfate.^{18, 28-30} All of these oxidants are capable of initiating PDA formation in slightly acidic environments, however each exhibits different kinetics.²⁸ Using SP, the solution can be oxidized to dopaminequinone within a few minutes,^{18,28} while polymerization using ammonium persulfate or copper sulfate takes longer.²⁸ Additionally, polymerization utilizing SP at a slightly acidic pH appears to form PDA that is structurally similar to PDA formed using atmospheric oxygen at an alkaline pH, while PDA formed with copper sulfate or ammonium persulfate was found to have more uncyclized species present.²⁸ For those reasons, we used SP as the oxidant in this study, with a slightly acidic acetate buffer in order to prevent a competing pathway with oxygen as the oxidant.

1.4 Coating Methods

1.4.1 Dip Coating

In addition to the choice of oxidant, buffer, and pH, PDA thin films can also be controlled through variations in deposition method. The original method used in the pioneering study by Lee et al. was dip coating,¹ wherein the substrate is submerged in the PDA solution for a determined amount of time until the film reaches the desired thickness (Figure 8). This method is ideal for unique shapes and small objects as the PDA solution can conform to nonuniform edges; however, this method generates a large amount of waste, as a sufficient amount of PDA solution to cover the entire object must be prepared. Dip coating can be

used in combination with any oxidant, as the substrate can simply be submerged for varying amounts of time to accommodate for a range of kinetics.

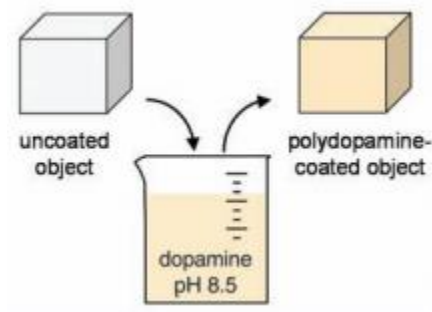


Figure 8. Original dip coating method used by Lee et al.¹

1.4.2 Spray Coating

Another common deposition method is spray coating. In this method, the DA solution and oxidant are sprayed onto a substrate, combining as they hit the surface (Figure 9).³¹ Unlike in dip coating, spray coating is limited to the use of strong oxidants as the PDA layer must be formed before the solvent evaporates off the substrate.³¹ Spray coating is useful in industrial applications and for coating large surface areas as it does not require excessive amounts of PDA solution or specialized equipment.³¹⁻³³ Both dip and spray coating have traditionally exposed the PDA solution to the substrate immediately after the solution is made.

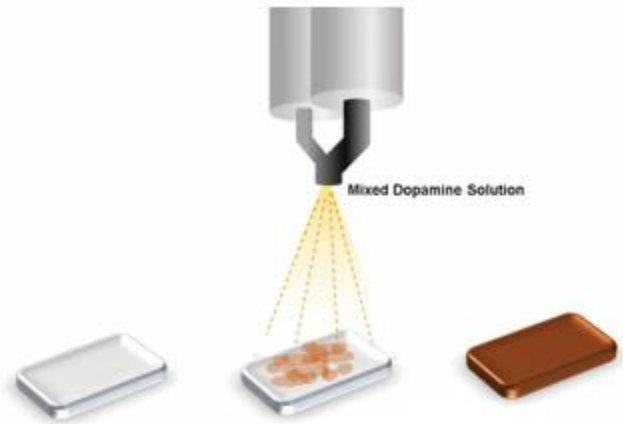


Figure 9. Spray coating method, as used by Hong et al.³¹

1.4.3 Spin Coating

The coating method used in this study is spin coating, which is used in multiple industries to apply a thin, uniform coating onto a planar surface.^{34, 35} The liquid deposited undergoes a four-step process of thin film formation: deposition, spin up, spin off, and solvent evaporation (Figure 10).³⁵ Unlike dip or spray coating, the aging time of the PDA solution can be altered in spin coating to visualize a snapshot of the adhesiveness of the solution at different times during polymerization. This is particularly useful given the complexities of PDA polymerization discussed earlier.

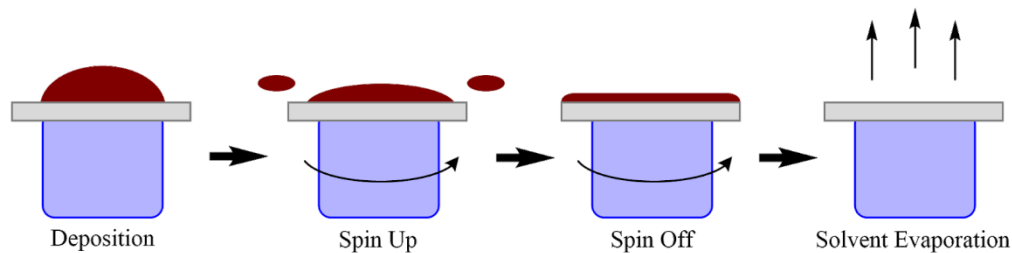


Figure 10. Schematic of the four steps of spin coating.

In order to ensure that our results using spin coating were applicable to other methods, we tested a modified dip coating method. This method used all of the same experimental parameters as spin coating, including allowing the solution to age before introducing it to the substrate and only allowing the substrate contact with the PDA solution for a set adhesion time of 1 min.

1.5 Substrate Chemistry

As discussed earlier, PDA is able to bind to many different substrates. However, the chemistry of the substrate yields differences in PDA thin film formation.³⁶ In this project SiO_2 , polydimethylsiloxane (PDMS), and 4-5% aminopropyl methylsiloxane – dimethylsiloxane copolymer (PADMS) were chosen in order to observe many types of potential interactions with PDA. SiO_2 is a base silicon wafer with no polymer coating. The surface of the wafer is studded with silanol groups, which are deprotonated at a neutral pH (Figure 11). This surface is hydrophilic, PDA can hydrogen bond with the silanol groups on

the wafer surface, and the negative charges on the surface can interact electrostatically with positively charged species in PDA (Table 2).¹⁸

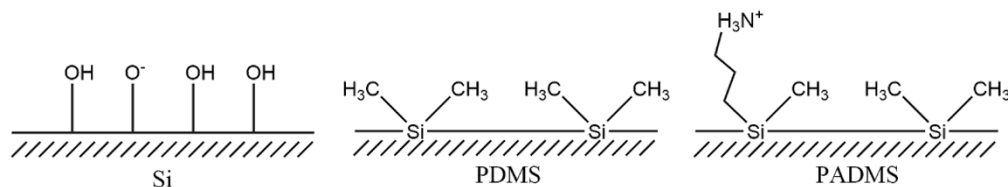


Figure 11. Chemical structures of the three substrates used in this experiment. The two polymer substrates were covalently adhered to a silicon wafer base.

Table 2. Substrates and their chemical interactions with PDA.¹⁸

Substrate	Types of interactions with PDA
SiO ₂	<ul style="list-style-type: none"> • Hydrogen Bonding • Electrostatic Interactions
PDMS	<ul style="list-style-type: none"> • Hydrophobic Interactions
PADMS	<ul style="list-style-type: none"> • Hydrophobic Interactions • Hydrogen Bonding • Electrostatic Interactions • Covalent Bonding • π-Cation Interactions

PDMS and PADMS are polymers with alternating silicon - oxygen backbones. PDMS has two methyl groups on each silicon atom (Figure 12). The structure of PDMS yields a polymer with unique properties. It has high thermal stability due to the large bond energies of the backbone, a low glass transition temperature of $-127\text{ }^{\circ}\text{C}$, and little energy is required to rotate the silicon - oxygen bonds in the backbone. This gives rise to larger bond angles than its carbon backbone counterpart.^{37, 38}

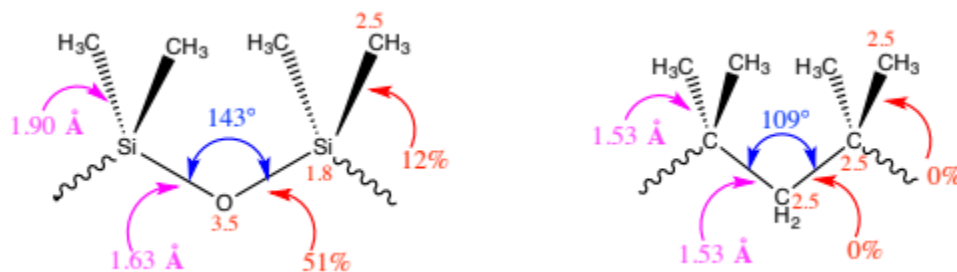


Figure 12. PDMS compared with its carbon backbone counterpart. Bond lengths are shown in pink, bond angles are shown in blue, electronegativity and percent ionic character are shown in red.³⁹

In order to be used as substrates, PDMS and PADMS are covalently attached to the base silicon wafer. These polymers are chemically very similar (Figure 11). The only difference in their structure is that PDMS is studded solely with methyl groups meaning that it can only interact with PDA via hydrophobic interactions (Table 2), while 2.5% of those methyl groups are replaced with propylamine groups in PADMS. This opens more possibilities for interactions with PDA, including hydrogen bonding, electrostatic

interactions, covalent bonding, and π -cation interactions in addition to the already present hydrophobic interactions (Table 2).

1.6 Project Overview

In this study, PDA thin films were spin cast onto SiO₂, PDMS, and PADMS in order to determine the differences in film thickness, contact angle, and surface morphology as a function of PDA aging times on different substrates. A slightly acidic acetate buffer and SP as an oxidizing agent were used in accordance with previous optimization research. Ellipsometry was used to determine film thickness, contact angle goniometry was used to determine advancing and receding contact angles, and atomic force microscopy (AFM) was used to determine surface morphology. It was found that the PDA films spin cast on PDMS and PADMS yield vastly different surface morphologies, despite the structural similarities of the polymers. Therefore, PADMS/PDMS polymer mixtures with a variety of volume ratios were also studied in order to determine the largest amount of PADMS that could be added while retaining the PDA morphology of that on pure PDMS. The volume fraction of PADMS present in the mixtures ranged from 3/4 to 1/200,000. In order to achieve a continuous film on pure PDMS, a 5x dilution of the acetate buffer was used to reduce the interference of salt ions in the adhesion process.

Additionally, a modified dip coating method was tested on SiO₂ samples where all the experimental variables were controlled between the modified dip

and spin coating other than the physical method of deposition. This confirmed that the coating method used does not prevent our conclusions from being more broadly applicable. An attempt was also made to “freeze” PDA solutions at their most adhesive state in order to prolong the usefulness of each solution. This was done by decreasing the pH of the solution in order to slow polymerization after allowing it to age to its most adhesive state. This did slow polymerization; however, it also decreased the adhesiveness of the solution, limiting its functionality for this application.

II. MATERIALS AND METHODS

2.1 Materials

Silicon wafers (100 orientation, P/B doped, resistivity 1-10 Ωcm , thickness 475-575 μm) were purchased from International Wafer Service. Polydimethylsiloxane, PDMS-T22 (MW: 9430 g/mol) and 4-5% aminopropyl methylsiloxane – dimethylsiloxane copolymer, PADMS-152 (MW: 7,000 - 9,000 g/mol) were purchased from Gelest. Dopamine hydrochloride (99.8%) was purchased from Sigma-Aldrich. Sodium periodate (SP) (99%) was purchased from Acros Organics. HPLC-grade toluene, acetone, and ethanol were purchased from Pharmco. Water was purified by Millipore Milli-Q Biocel System (Millipore Corp., resistivity $\geq 18.2 \text{ M}\Omega/\text{cm}$). Glacial acetic acid (ACS reagent grade), sodium acetate trihydrate ($\geq 99\%$), sodium chloride (ACS reagent grade) and 0.1 M hydrochloric acid (ACS reagent grade) were purchased from Fisher Scientific, Inc. Oxygen and nitrogen gases (99.999%) were purchased from Middlesex Gases Technologies.

2.2 Preparation of DA solutions

A solution of dopamine hydrochloride and SP, with $[DA] = 4 \text{ mg/mL}$ and $[SP]:[DA] = 2$, was prepared in a 50-mL centrifuge tube. SP was dissolved first in a 0.25 M pH 5.9 acetate buffer using a vortex mixer until fully dissolved (approximately 30 s). Dopamine hydrochloride was then dissolved in the solution with a vortex mixer for 5-10 s. Reaction time was measured from the moment that dopamine hydrochloride was added to the solution.

2.3 Substrate Preparation

2.3.1 SiO₂

Silicon wafers were cut into 1.4 x 1.4 cm squares using a diamond tipped cutter. The wafers were rubbed with clean, gloved hands under distilled water, then dried using compressed air. They were then placed in a Precision 51221126 Gravity Convection Lab Oven (Thermo Fisher Scientific, Inc) for half an hour at 110 °C to dry completely. After cooling to room temperature, the wafers were cleaned using oxygen plasma in a PDC-001 Harrick plasma cleaner (Harrick Scientific Products, Inc., USA) for 15 min at 300 mTorr and 30 W. They were then left to equilibrate for 15 min, covered and under ambient pressure, to prevent contamination from dust particles.

2.3.2 PDMS and PADMS

To prepare PDMS and PADMS wafers, each wafer was placed into an individual scintillation vial after equilibration. 100 μ L of polymer was added on top of each wafer. The wafers were then heated at 100 °C using a 150-timer heater (J-KEM Scientific, Inc.) for 24 h. After cooling to room temperature, the wafers were rinsed sequentially with toluene, acetone, and Milli-Q water to remove excess polymer. After rinsing, the wafers were dried with nitrogen gas, then stored in a desiccator overnight before characterization or PDA adhesion.

2.3.3 PADMS-PDMS Mixtures

PADMS polymer was diluted by volume with PDMS and mixed using a vortex mixer for approximately 30 s. Serial dilution was used for fractions of PADMS smaller than 1/4. Substrates containing PADMS-PDMS mixtures were prepared following the same procedure as that for PADMS and PDMS substrates.

2.4 Coating Methods

2.4.1 Spin Coating

A wafer sample was placed on the stage of a Laurell WS-650MZ-23NPPB spin coater. The sample was held in place by vacuum and the spin coater was kept under nitrogen gas to minimize atmospheric interference. After

a reaction time of up to 30 min, a drop of 4 mg/mL PDA solution ([SP]:[DA] = 2) was placed onto the wafer (100 μ L for SiO₂, 500 μ L for PDMS, PAMS, and PAMS-PDMS wafers). The PDA solution was allowed an adsorption time of one minute on the wafer. The sample was then spun for one minute at 6000 rpm. Immediately after spin coating, the wafers were rinsed with Milli-Q water on both sides for approximately 10 s each side. Excess water was removed by placing the edge of the wafer onto a Kimwipe. The wafers were then stored in a desiccator overnight before characterization.

2.4.2 Modified Dip Coating

Wafer samples were placed in individual wells in a 24 well plate. After a reaction time of up to 30 min, 4 mg/mL PDA solution ([SP]:[DA] = 2) was placed into the well to cover the entire sample. The sample was allowed an adsorption time of one minute in the PDA solution. The well was then flushed with Milli-Q water and the sample was removed. Immediately after removal from the well, the wafers were rinsed with Milli-Q water on both sides for approximately 10 s each side. Excess water was removed by placing the edge of the wafer onto a Kimwipe. The wafers were then stored in a desiccator overnight before characterization.

2.5 Characterization Methods

2.5.1 Thickness

The thickness of wafers was measured using an LSE Stokes ellipsometer (Gaertner Scientific) equipped with a 1 mW He-Ne laser (wavelength 632.8 nm). The measurement error is within 1 Å. Each wafer was measured in four arbitrary locations. The thickness of PDA was extrapolated by subtracting the thickness of the substrate from each PDA-coated sample.

2.5.2 Contact Angle

Both advancing and receding dynamic contact angles on each sample were measured using Milli-Q water with a Gilmont syringe (Gilmont Instrument Co.) and a 24-gauge flat-tipped needle. They were digitally analyzed by a NRL CA 100-00 telescopic goniometer (Rame-Hart Instrument Co.) . Measurements were carried out in four arbitrary locations on each wafer.

2.5.3 Atomic Force Microscopy

Nanoscopic surface topography images were taken by a Veeco Metrology Dimension 3100 atomic force microscope (AFM) in tapping mode. Image analysis was conducted using Nanoscope software (Veeco Instruments, Inc.).

2.5.4 Optical Microscopy

Optical images were taken using a Brightfield Olympus BX51 optical microscope in reflective mode.

III. RESULTS AND DISCUSSION

In order to determine how PDA thin film formation was affected by substrate chemistry, PDA was spin cast on a hydrophilic substrate, SiO₂, a hydrophobic substrate with methyl groups, PDMS, and a hydrophobic substrate with methyl and amine groups, PADMS. For each substrate, PDA was spin cast after a range of aging times in order to determine the time point with the most adhesive species present in solution, which is indicated by a maximal thickness and continuous PDA coverage shown in AFM images.

3.1 Substrate Chemistry

The three substrates were chosen to offer a range of chemical properties and possible interactions with PDA. SiO₂, the surface layer of a clean silicon wafer, has a thickness of 1.0 nm and low advancing and receding contact angles (Table 3). These low contact angles are indicative of its hydrophilicity which is expected from the silanol groups on its surface (Figure 11). Both PDMS and PADMS are polymers which are covalently adhered to clean silicon wafers in order to be used as substrates. Both polymers are composed of a silicon-oxygen backbone. When adhered to silicon wafers they present very similar thicknesses

(Table 3). PDMS only has methyl group substituents which makes it a hydrophobic surface, as shown in its high contact angles (Table 3). In PADMS, 2.5% of the methyl groups have been exchanged with amine groups. This lowers the hydrophobicity slightly, which is reflected in the slightly lower contact angles of PADMS as compared to PDMS (Table 3).

Table 3. Substrate thickness and contact angle.

Substrate	Thickness (nm)	Contact Angle (°)
SiO ₂	1.0 ± 0.2	$30 \pm 4/4 \pm 1$
PDMS	5.9 ± 0.6	$111 \pm 1/98 \pm 1$
PADMS	5.8 ± 0.2	$107 \pm 1/80 \pm 2$

3.2 Spin Coating PDA at Various Aging Times

3.2.1 Thickness and Contact Angle

SiO₂, PDMS, and PADMS wafers were spin coated with PDA after an aging time ranging from 1-30 min. For all substrates, the thickness of the PDA layer increased up to a certain time point and then dropped back down. The PDA layer on PADMS and PDMS reached a maximum thickness at 2 min, while on SiO₂ the maximum was at 5 min (Figure 13). This result is mirrored in the contact angles. Both PDMS and PADMS with no PDA coating have

advancing contact angles above 100° , and when spin coated with dopamine the contact angles drop to their lowest points at 2 min (Figures 14, 15). SiO_2 has a low advancing contact angle without modification, and when spin coated with dopamine the advancing contact angle reaches its peak at 5 min (Figure 14). For both SiO_2 and PADMS, the receding contact angle stays consistent throughout all time points (Figure 14), but for PDMS, the receding contact angle also has a minimum at 2 min, which indicates that at low PDA thicknesses the sample has fewer hydrophilic groups present at the surface (Figure 15).

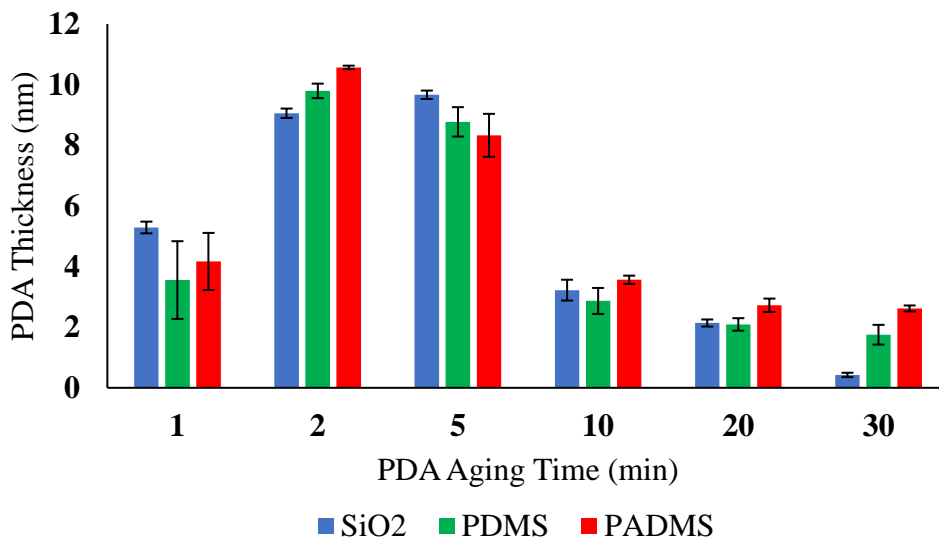


Figure 13. Thickness of PDA on all substrates. Time indicates the aging time of the DA solution from the point when dopamine hydrochloride was added until the solution was introduced to the substrate. For all samples, the DA solution was in contact with the substrate for 1 min before spin.

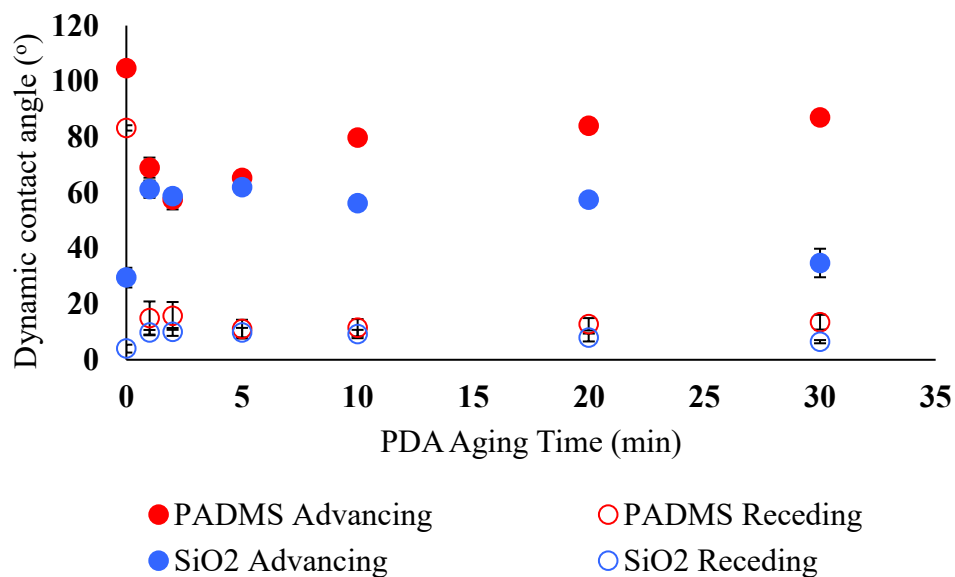


Figure 14. Advancing and receding dynamic contact angles of PDA on PADMS and SiO₂. The 0 time point indicates the contact angles of the substrates with no PDA.

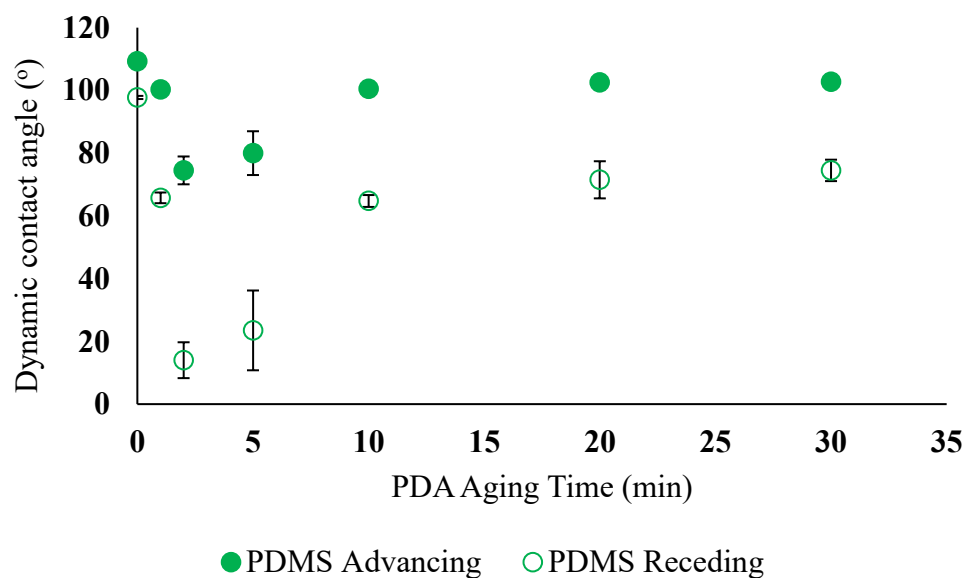


Figure 15. Advancing and receding dynamic contact angles of PDA on PDMS. The 0 time point indicates the contact angles of unmodified PDMS.

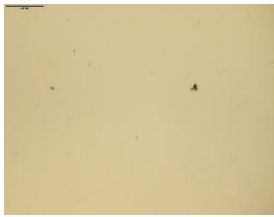
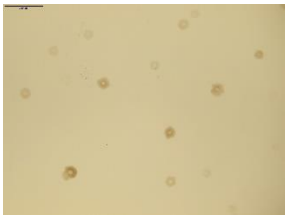







The extrema in thickness and contact angles indicate that the aging time of PDA solution plays a significant role in the ability of PDA to adhere to a substrate. There appears to be a critical time point when PDA is best able to adhere, although this differs slightly with different substrates. The thickest layer of PDA adheres to the hydrophobic polymers after 2 min of aging, while for the hydrophilic SiO₂, the thickest layer of PDA adheres after 5 min of aging. Although it is not necessarily only the hydrophobicity of the substrates causing this change, it is important to note that the critical aging time is dependent on the substrate PDA is adhering to and is therefore not entirely an intrinsic property of PDA itself. The existence of a peak aging time is most likely due to the concentrations of different adhesive species and the size of the PDA particles changing over time.¹⁸ As the solution ages, particles of PDA are formed which grow and eventually precipitate out of solution. Larger particles adhering to the substrate cause a thicker film, however as more particles precipitate out of solution, they are no longer able to be transferred onto the substrate. Additionally, as the particles become too large, they are spun off during the coating process. These both contribute to the decrease in thickness at longer aging times.

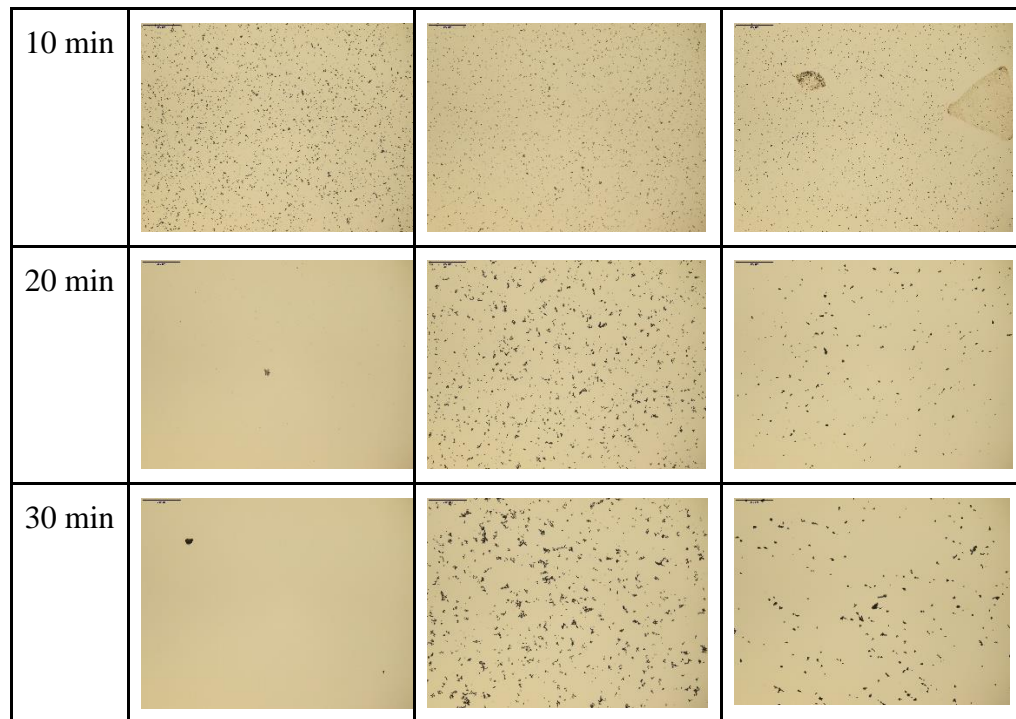
3.2.2 Optical Microscopy

Additionally, the number of large particles adhered to the substrates does not directly correlate with the thickness, as shown in optical microscopy

images. There are large, visible particles at 10 min on all three substrates, and at longer aging times on PADMS and PDMS (Table 4). This does not line up with the peak thicknesses observed for the substrates at 5 and 2 minutes (Figure 13). Since the density of large particles on the surface is relatively low, they do not form a cohesive film, meaning that the PDA thickness is also low despite the presence of some large particles on the surface.

Table 4. Optical images at 10x magnification of PDA on all substrates as a function of PDA aging time, with a scale bar of 200 μm .

Time	SiO ₂	PADMS	PDMS
1 min			
2 min			
5 min			





















3.2.3 Atomic Force Microscopy

Another difference between the substrates is most clearly demonstrated with AFM. The growth mechanism of PDA on SiO_2 and PADMS appears similar with small dots at very low and very high aging times, and larger dots at a higher density near the critical aging time, with complete coverage at all time points (Table 5). The growth mechanism on PDMS is very different. “Islands” of PDA with “cracks” separating them become larger up to the critical aging time, after which the islands become small again (Table 5). This is consistent with the receding contact angles. The rough PDA surface with exposed PDMS at very short and very long aging times is consistent with larger

receding contact angles, while the smooth layer of PDA present on SiO₂ and PADMS for all aging times is consistent with smaller receding contact angles.

Table 5. AFM images (size: 1.25 x 5 μm^2 , height scale: 20 nm) of PDA on all substrates as a function of PDA aging time.

Time	SiO ₂	PADMS	PDMS
1 min			
2 min			
5 min			
10 min			
20 min			
30 min			

This difference in growth mechanism is most likely due to the types of interactions that PDA is able to have with each substrate. SiO₂ is able to form hydrogen bonds and can have electrostatic interactions with PDA, while the amine groups on PADMS allow for hydrogen bonding, electrostatics, π -cation interactions, and covalent bonding in addition to the hydrophobic interactions with the bulk of the polymer. Alternatively, PDMS is only able to form hydrophobic interactions with PDA. This could explain why PDA only adheres to PDMS in islands. Since it lacks the ability to form stronger interactions, it

would need a buildup of many hydrophobic interactions in order to adhere securely to the substrate, and it can maximize these interactions by PDA particles spreading and adhering in this island morphology.

This is an especially interesting observation, as PDMS and PADMS are very similar in structure, with the only difference being that PDMS contains all methyl groups, while PADMS contains 97.5% methyl groups and 2.5% amine groups. In order to determine the amount of amine groups necessary for PDA to adhere in the same manner as on PADMS and SiO_2 , we diluted PADMS with PDMS by volume before reacting the mixtures with the wafers. The fractions presented are the fraction of PADMS in the mixtures, and therefore may not be entirely representative of the percent of amine groups which are actually present on a substrate surface.

3.3 Spin Coating PDA on Substrates Containing PADMS and PDMS Mixtures

3.3.1 Thickness

In order to best visualize the growth mechanism, the substrates containing the polymer mixtures were spin cast with PDA after 1 min of aging time, since this is shorter than the critical aging time for both PADMS and PDMS. The thickness of PDA remained 4-7 nm for all polymer mixtures (Figure 16), which was expected since the thickness of PDA spin cast at 1 min is similar for both PDMS and PADMS.

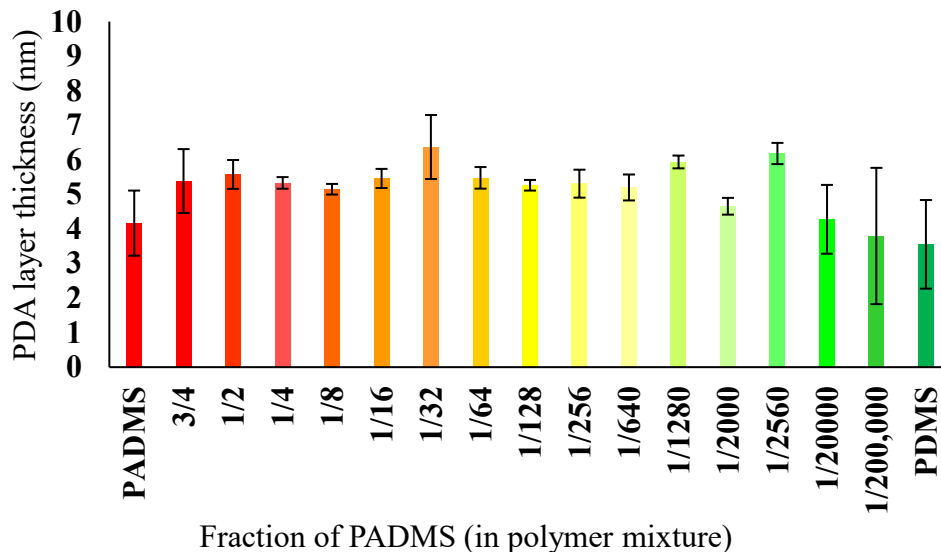
















Figure 16. Thickness of PDA on substrates containing polymer mixtures as a function of fraction of PADMS in polymer mixture.

3.3.2 Atomic Force Microscopy and Contact Angle

The AFM images show that the growth mechanism remains the same as pure PADMS until the PADMS volume fraction is reduced to 1/640 when small cracks become visible (Table 6). These cracks become larger and more obvious when the PADMS fraction is reduced to 1/20,000 and resemble the island morphology on PDMS when the PADMS fraction is 1/200,000. This is reflected in the dynamic contact angle data, which also show a transition in the advancing and receding contact angles of PDA when the PADMS fraction is 1/20,000 (Figure 17). However, the dynamic contact angles of the unmodified polymer substrates show a shift much earlier, with distinct contact angles from pure PADMS to the composite substrate containing 1/16 of PADMS (Figure

18). This shows that the surface of the mixed polymers is chemically distinct from pure PADMS, however, it is not until PADMS is diluted to 1/20,000 that it is distinct enough for PDA to adhere in a similar manner to PDMS.

Table 6. AFM images (size: $1.25 \times 5 \mu\text{m}^2$, height scale: 20 nm) of PDA spin cast after 1 min aging time on polymer mixtures. The different polymer compositions are represented by the volume fraction of PADMS present.

PADMS		1/256	
3/4		1/640	
1/2		1/1280	
1/4		1/2560	
1/16		1/20,000	
1/64		1/200,000	
1/128		PDMS	

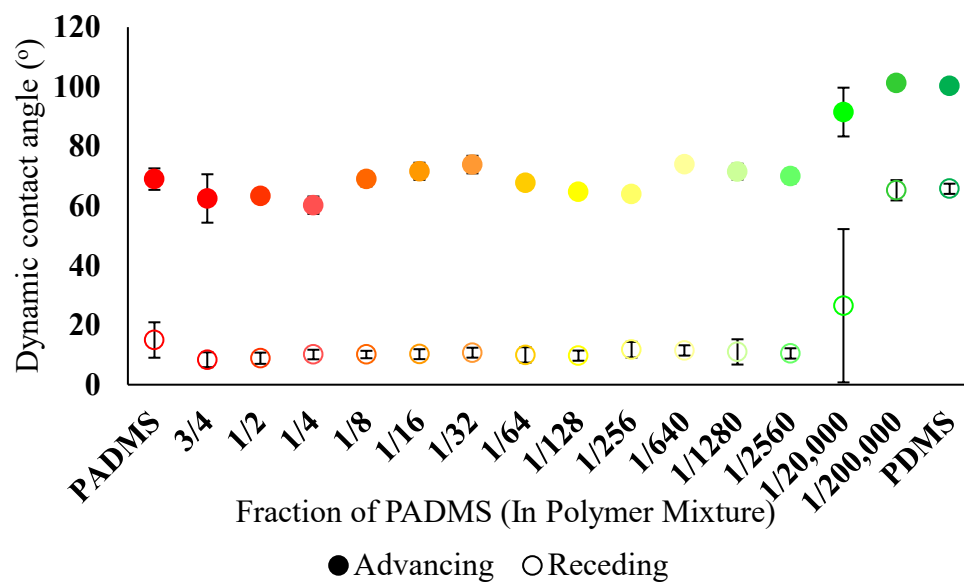


Figure 17. Advancing and receding dynamic contact angles of PDA spin cast after 1 min aging time on substrates containing polymer mixtures.

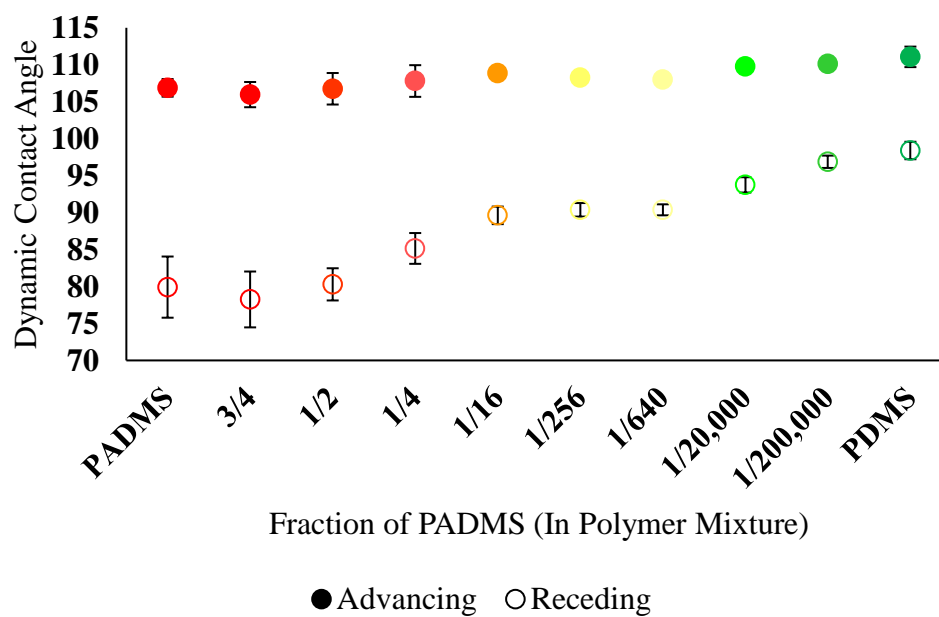


Figure 18. Advancing and receding dynamic contact angles of substrates containing polymer mixtures.

This indicates that only a very small amount of PADMS is sufficient for PDA to adhere with the same mechanism as on pure PADMS. Although there is very little amine present in the diluted mixtures of polymer, it is unclear how much amine is present on the substrate surface. As the polymer is covalently attached to the surface of the silicon wafer, electrostatic interactions between the negatively charged silanol groups and the positively charged amine groups could cause the percent of amine groups in solution to be an underestimation of the amine groups present on the surface. However, since the contact angles of the polymer mixtures with no PDA present are distinct from one another at higher PADMS concentrations, it is clear that the chemical makeup of the surface is changing as the PADMS is diluted with PDMS. Future research using X-ray photoelectron spectroscopy could help to elucidate this.

3.4 Buffer Dilution

3.4.1 Thickness

In order to achieve a continuous film on pure PDMS, we performed a 5x dilution of the acetate buffer before dissolving SP and DA into solution. With a reduced salt concentration, the PDA would have greater access to the substrate since there would be less interference from salt ions. The thickness shows a similar trend as the undiluted buffer system; however, the peak thickness is delayed to 5 min (Figure 19). This can be explained by Le

Chatelier's principle. In reducing the buffer capacity, the pH of the solution dropped farther than the undiluted buffer system with the addition of DA. This increase in proton concentration would be sufficient to slow the polymerization reaction of DA.

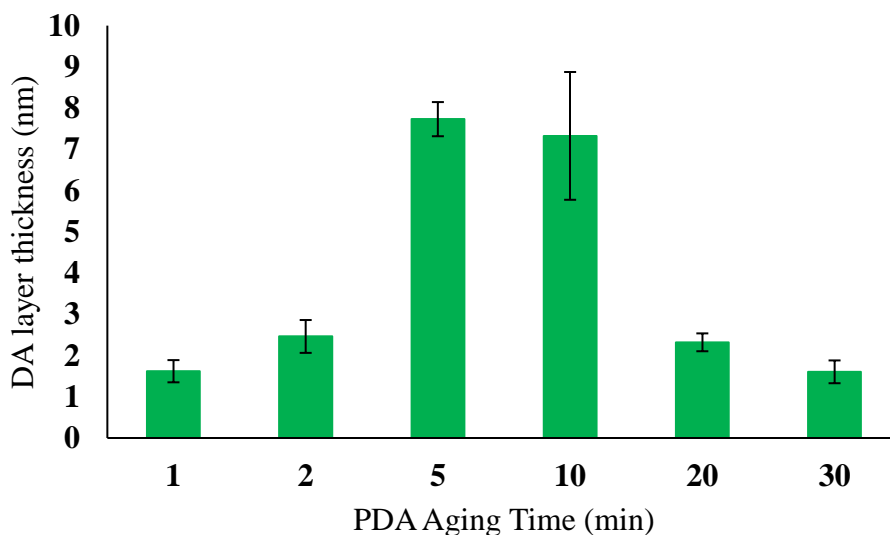



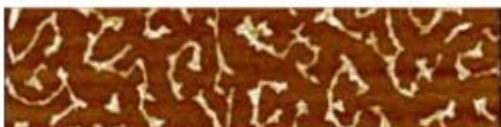

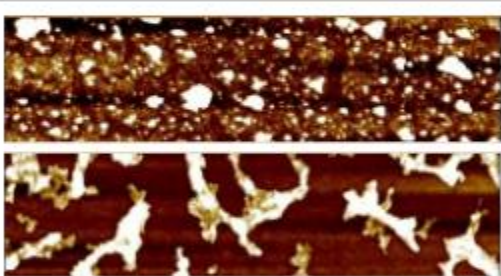


Figure 19. Thickness of PDA on PDMS as a function of aging time, using a 5x diluted buffer solution.

3.4.2 Atomic Force Microscopy and Contact Angle

Although the same growth mechanism as undiluted buffer is present, complete coverage was achieved at 5 min aging time (Table 7). 10 min aging time, which has a similar thickness to 5 min (Figure 19), shows close to complete coverage with larger PDA particles present in certain areas, although cracks are visible elsewhere on the wafer (Table 7). The contact angles reinforce this, with the lowest point at 5 min aging time (Figure 20). The contact angles

at 10 min aging time have exceptionally large standard deviations which comes from the range of morphologies present on the sample (Figure 20).

Table 7. AFM images (size: $1.25 \times 5 \mu\text{m}^2$, height scale: 20 nm) of PDA spin cast on PDMS using a 5x diluted buffer solution.

1 min	
2 min	
5 min	
10 min	
20 min	
30 min	

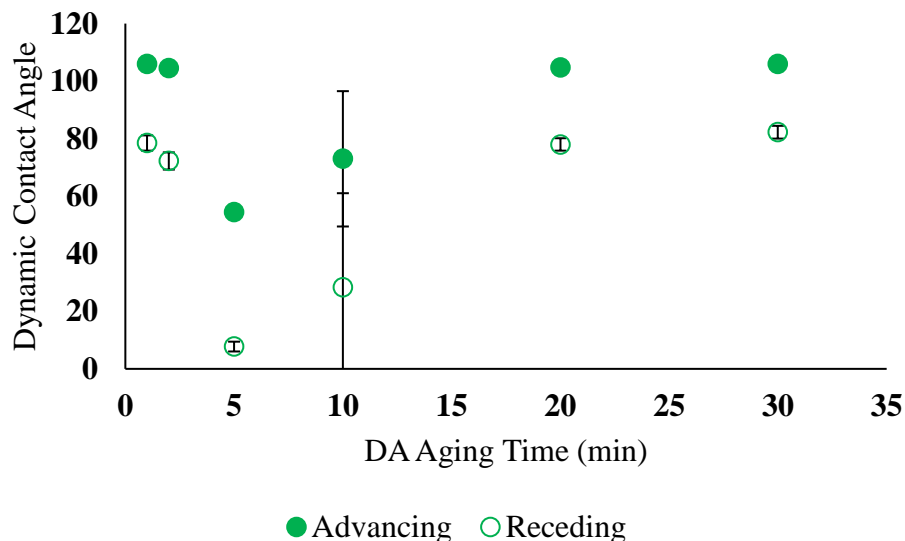


Figure 20. Advancing and receding dynamic contact angles of PDA on PDMS using a 5x diluted buffer solution.

3.5 Modified Dip Coating

3.5.1 Thickness and Contact Angle

As previously discussed, there are a myriad of experimental factors that can affect the properties of PDA thin films. Since dip coating is the traditional method of PDA adhesion, we created a modified dip coating method in order to confirm that the conclusions reached via spin coating are applicable to other coating methods. This method controls for the differences in PDA application between dip and spin coating by creating a dip coating application method using the experimental factors present in spin coating. Crucially, the PDA solution was allowed to age before being introduced to the substrate for 1 min. This is altered from traditional dip coating where the substrate is exposed to PDA at

aging time 0 and allowed to be in contact with the substrate until the desired adhesion time.

The thickness using the modified dip coating on SiO₂ had a maximum thickness at the same aging time as spin coating, although overall the thicknesses for modified dip coating were lower (Figure 21). This could be due to the types of particles that the substrate is exposed to with the different methods. In the modified dip coating method, the substrate is exposed to all types of PDA particles present in the solution. For spin coating, only the particles which are transferred via pipette are exposed to the substrate. If less adhesive PDA particles are present low in the solution, they could potentially block more adhesive species from reaching the substrate. Additionally, the adhesion time for modified dip coating is slightly longer than 1 min since it takes time for the excess PDA solution to be removed from the substrate.

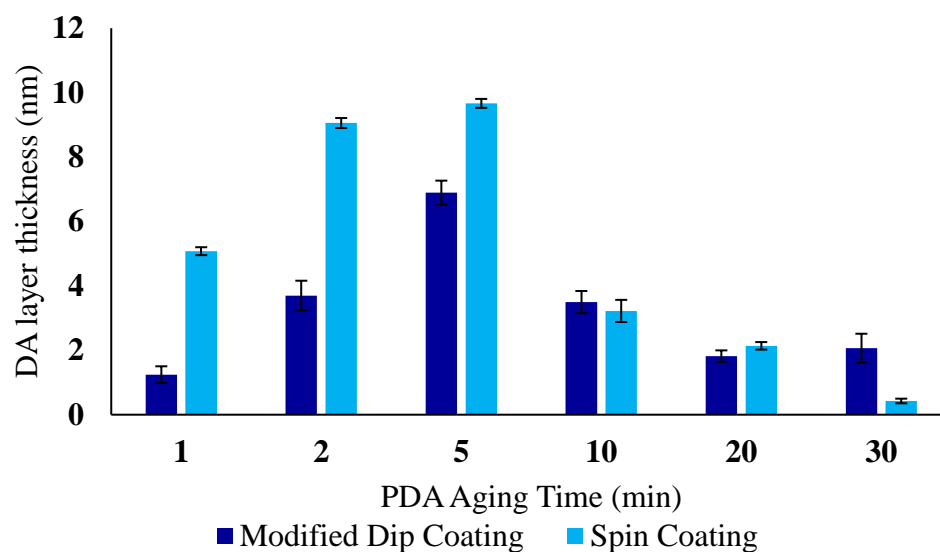


Figure 21. Thickness of PDA on SiO₂ using both modified dip and spin coating as a function of PDA aging time.

The contact angles for both modified dip and spin coating look very similar up until a PDA aging time of 30 min (Figure 22). This discrepancy can be explained by the very low thickness for spin coating at this time point (Figure 21).

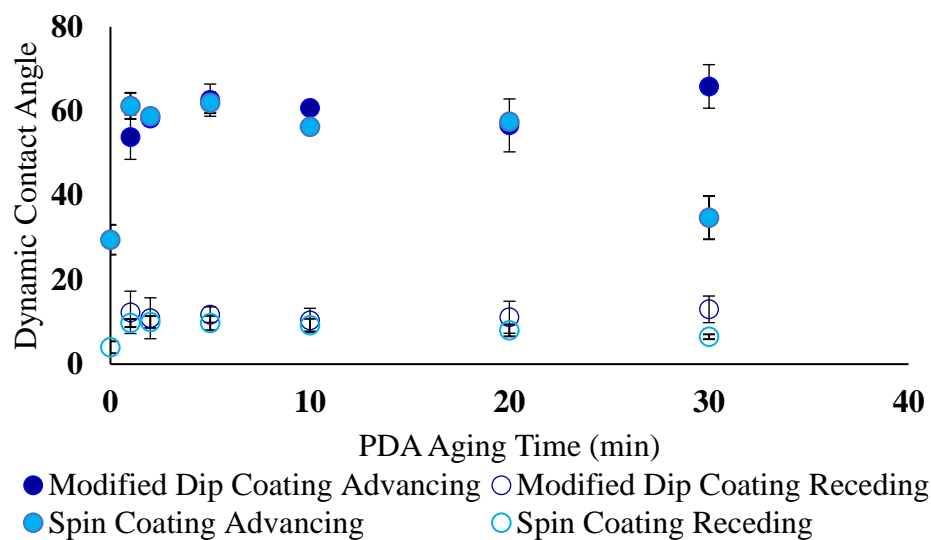


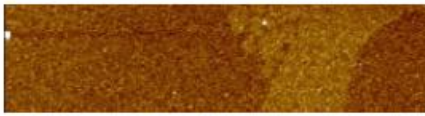
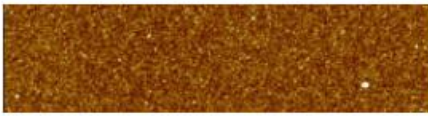

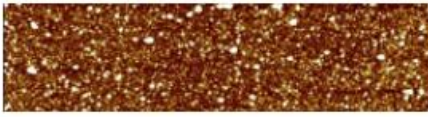
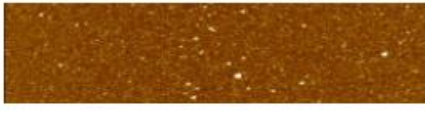







Figure 22. Dynamic contact angles of PDA on SiO₂ using modified dip and spin coating as a function of PDA aging time.

3.5.2 Atomic Force Microscopy

The AFM images of PDA on SiO₂ looked virtually identical with both modified dip and spin coating (Table 8). At the peak aging time of 5 min, spin coating yielded slightly larger particles which is consistent with the thickness data.

Table 8. AFM images (size $1.25 \times 5 \mu\text{m}^2$, height scale: 20 nm) of PDA on SiO_2 using modified dip and spin coating.

	Modified Dip Coating	Spin Coating
1 min		
2 min		
5 min		
10 min		
20 min		
30 min		

Overall, both spin and modified dip coating showed a maximum thickness at the same aging time and similar contact angle and AFM data. Therefore, it is reasonable to assume that discrepancies between traditional dip and spin coating is due to altered experimental factors rather than the coating method itself. Crucially, this means that conclusions drawn from this project are relevant to studies which use dip coating.

3.6 “Freezing” PDA

Since there is an optimal PDA aging time for adhesion, we wanted to see if it was possible to “freeze” the PDA polymerization process at that time point in order to be able to use a single PDA solution over a longer period of time. Since low pH causes the polymerization reaction to slow considerably, we decided to add concentrated HCl to lower the pH and stop polymerization at the optimal aging time.

We chose PADMS as a test substrate for these trials since it can be stored for longer than SiO₂ and does not have the growth mechanism complications of PDMS. For the first trial, we added 20 $\mu\text{L/mL}$ of concentrated HCl after letting the PDA solution age for 2 min. Due to the adhesive nature of PDA at this aging time, the exact pH could not be determined accurately without damage to the pH meter. The PDA did not adhere well at any of the time points tested (Figure 23), indicating that the pH was too low for adequate adhesion. We then lowered the amount of HCl added to 15 $\mu\text{L/mL}$ in order to test if a smaller pH decrease would increase adhesion. The addition of less HCl did allow for more adhesion, however there is still a maximum thickness point at 10 min after adding HCl (Figure 23). This indicates that the PDA formation was slowed after HCl was added, but the PDA particles were not frozen in their most adhesive state as intended.

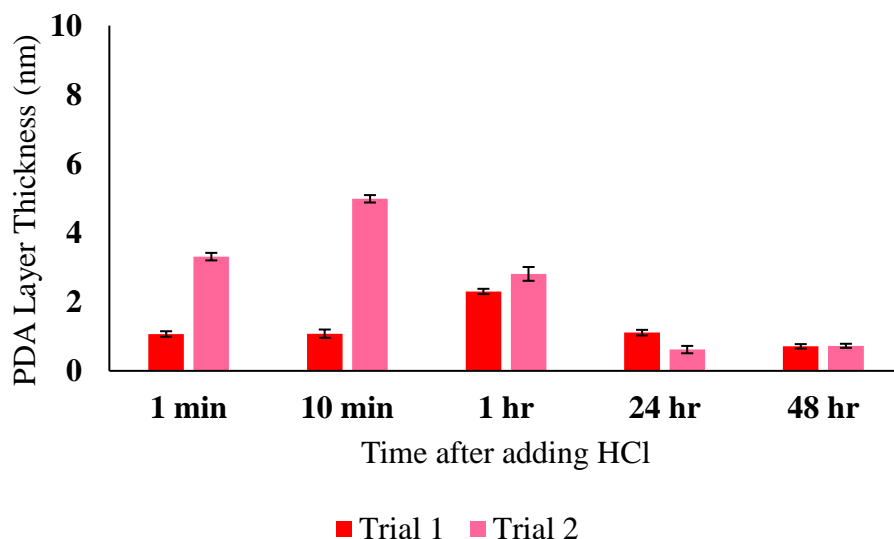


Figure 23. Thickness of PDA on PADMS as a function of time after HCl was added to the PDA solution.

Given the complexities in dopamine polymerization as well as the high propensity for PDA particles to stick to each other in solution, extending the shelf life of PDA solutions is a complex problem. Despite the inherent challenge it poses, a method to halt PDA polymerization while in its most adhesive state would allow for less waste product and simplify the coating process. Therefore, future research into solving the problems laid out here could prove fruitful.

IV. CONCLUSIONS & FUTURE WORK

Under the conditions presented, PDA exhibits a maximum adhesiveness at a peak aging time on each substrate examined, with the thickest and most continuous PDA films yielded at that time point. For PDMS and PADMS, this peak aging time is about 2 min, while for SiO₂ it is about 5 min. Since the structure of PDA changes over time, the variation in thickness at different time points indicates that particle size and chemical composition are extremely important to PDA adhesion. The variation in peak aging time for the different substrates indicates that ideal adhesive conditions are slightly substrate dependent.

The substrate dependency of PDA can be clearly seen when examining the growth mechanism of PDA on PDMS and PADMS. Although the two polymers are structurally similar, the presence of a small amount of amine groups on the surface of PADMS causes PDA to adhere in different morphologies on each polymer. The amine groups on the surface of PADMS allow PDA to adhere using many different chemical interactions. This causes PDA to form a continuous film on PADMS even at low thicknesses. This contrasts with the adhesion of PDA on PDMS. Since PDA can only adhere to

PDMS via hydrophobic interactions, it forms films which have large cracks at low thicknesses in order to maximize those interactions. These cracks become smaller as the film thickness increases.

Since the presence of amine groups is the only thing that differentiates PADMS from PDMS, we diluted PADMS with PDMS in order to determine the amount of amine necessary on the substrate surface for PDA to form a continuous film at low thicknesses. We observed that PDA did not have clearly visible cracks until a PADMS volume fraction of 1/20,000. PDA exhibited large cracks similar to pure PDMS at 1/200,000. The PDA films on substrates with PADMS concentrations greater than 1/20,000 showed continuous coverage on AFM images and yielded similar advancing and receding contact angles to PDA on pure PADMS.

The contact angles of the substrates with no PDA adhered were visually distinct from pure PADMS well before the 1/20,000 threshold. This indicates that the concentration of amine groups on the substrate surface decreases as the fraction of PADMS present decreases, however, until 1/20,000 parts PADMS the amount of amine groups present is still sufficient for PDA to adhere in a continuous film. Since the amine groups in PADMS are positively charged and the silicon wafer that it is adhered to has a surface with negatively charged silanol groups, it is possible that the true amount of amine groups present on the substrate is greater than that in the polymer

mixture. Future research using X-ray photoelectron spectroscopy could help to determine the actual chemical composition of the various polymer mixtures when they are adhered to the wafers. Additionally, spin coating PDA on substrates which are only capable of interacting with PDA via hydrogen bonding or π -cation interactions could provide insight into which interactions allow for continuous coverage in the presence of amine groups.

In addition to aging time and substrate chemistry, buffer, in terms of both pH and salt concentration, also plays an important role in PDA adhesion. On pure PDMS, we were able to achieve continuous PDA coverage at high thicknesses by using a 5x diluted buffer solution. This is most likely due to a reduction in salt ion concentration, which allows PDA easier access to the substrate. However, since the buffer capacity was reduced, the solution became more acidic, which slowed the polymerization reaction. This caused the aging time corresponding to the maximum thickness to be 5 min rather than 2 min.

Since the traditional method of PDA adhesion is dip coating, a modified dip coating method was used to control for the experimental differences between dip and spin coating. We were able to achieve similar results on SiO₂ using both spin and modified dip coating. This indicates that differences between the two coating methods are caused by other

experimental factors rather than the coating method itself, and conclusions drawn using spin coating may be used to inform other coating methods.

It is clear from this research that PDA has a peak aging time when the most adhesive species are present. Since reducing the pH of the solution slows polymerization, we attempted to reduce the pH of the PDA solution after it had reached the peak aging time in order to extend the lifespan of a single solution. With both trials, we found that adding HCl to the solution caused PDA to become much less adhesive. We also observed a peak thickness over the time points tested, meaning that the polymerization reaction was merely slowed rather than halted. Since PDA contains such adhesive species especially at its peak aging time, extending the lifespan of the most adhesive PDA solutions so that less material is wasted is a complicated problem, however, the ability to reuse PDA solutions would reduce waste material and simplify the adhesion process, so it would be beneficial to explore further in future research.

Overall, this research has demonstrated the importance of substrate chemistry and PDA aging time to thin film formation. Changing these two variables allows for a range of thicknesses and multiple thin film morphologies. This increases the versatility of PDA as a coating and means that the insights gained here will be beneficial to future applications, since the

deposition conditions can be tailored to the specific surface chemistry needs of future research.

REFERENCES CITED

1. Lee, H.; Dellatore, S. M.; Miller, W. M.; Messersmith, P. B. Mussel-Inspired Surface Chemistry for Multifunctional Coatings. *Science* **2007**, *318*, 426-430.
2. Brubaker, C.; Messersmith, P. The Present and Future of Biologically Inspired Adhesive Interfaces and Materials. *Langmuir* **2012**, *28*, 2200-2205.
3. Kord Forooshani, P.; Lee, B. P. Recent approaches in designing bioadhesive materials inspired by mussel adhesive protein. *J. Polym. Sci. Part A: Polym. Chem.* **2017**, *55*, 9-33.
4. Saiz-Poseu, J.; Mancebo-Aracil, J.; Nador, F.; Busqué, F.; Ruiz-Molina, D. The Chemistry behind Catechol-Based Adhesion. *Angew. Chem. Int. Ed.* **2019**, *58*, 696-714.
5. Ryu, J. H.; Messersmith, P. B.; Lee, H. Polydopamine Surface Chemistry: A Decade of Discovery. *ACS Appl. Mater. Interfaces* **2018**, *10*, 7523-7540.
6. Cui, M.; Ren, S.; Wei, S.; Sun, C.; Zhong, C. Natural and Bio-Inspired Underwater Adhesives: Current Progress and New Perspectives. *APL Mater.* **2017**, *5*, 116102.
7. Waite, J. Mussel Adhesion - Essential Footwork. *J. Exp. Biol.* **2017**, *220*, 517-530.
8. Yang, H.; Waldman, R. Z.; Wu, M.; Hou, J.; Chen, L.; Darling, S. B.; Xu, Z. Dopamine: Just the Right Medicine for Membranes. *Adv. Funct. Mater.* **2018**, *28*, 1705327.
9. Ball, V. Physicochemical perspective on “polydopamine” and “poly(catecholamine)” films for their applications in biomaterial coatings (Review). *Biointerphases* **2014**, *9*, 030801.
10. Ambrico, M.; Ambrico, P. F.; Cardone, A.; Della Vecchia, N. F.; Ligonzo, T.; Cicco, S. R.; Talamo, M. M.; Napolitano, A.; Augelli, V.; Farinola, G. M.; d’Ischia, M. Engineering polydopamine films with

- tailored behaviour for next-generation eumelanin-related hybrid devices. *J. Mater. Chem. C* **2013**, *1*, 1018–1028.
11. Cui, J. W.; Wang, Y. J.; Postma, A.; Hao, J. C.; Hosta-Rigau, L.; Caruso, F. Monodisperse polymer capsules: Tailoring size, shell thickness, and hydrophobic cargo loading via emulsion templating. *Adv. Funct. Mater.* **2010**, *20*, 1625–1631.
 12. Ho, C. C.; Ding, S. J. The pH-controlled nanoparticles size of polydopamine for anti-cancer drug delivery. *J. Mater. Sci.: Mater. Med.* **2013**, *24*, 2381–2390.
 13. Yang, J.; Cohen Stuart, M. A.; Kamperman, M. Jack of all trades: versatile catechol crosslinking mechanisms. *Chem. Soc. Rev.* **2014**, *43*, 8271–8298.
 14. Wagreich, H.; Nelson, J. M. On the oxidation product of catechol when oxidized by means of tyrosinase. *J. Biol. Chem.*, **1936**, *115*, 459–465.
 15. Felix, C. C.; Sealy, R. C. o-Benzosemiquinone and its metal chelates. Electron spin resonance investigation of radicals from the photolysis of catechol in the presence of complexing metal ions. *J. Am. Chem. Soc.*, **1982**, *104*, 1555–1560.
 16. Felix, C. C.; Sealy, R. C. Photolysis of melanin precursors: formation of semiquinone radicals and their complexation with diamagnetic metal ions. *Photochem. Photobiol.*, **1981**, *34*, 423–429.
 17. Ball, V.; Del Frari, D.; Toniazzo, V.; Ruch, D. Kinetics of Polydopamine Film Deposition as a Function of pH and Dopamine Concentration: Insights in the Polydopamine Deposition Mechanism. *J. Colloid Interface Sci.* **2012**, *386* (1), 366–372.
 18. Le, M. L.; Zhou, Y.; Byun, J.; Kolozsvari, K.; Xu, S.; Chen, W. Using a Spin-Coater to Capture Adhesive Species during Polydopamine Thin Film Fabrication. *Langmuir*, **2019**, *35*, 12722–12730.
 19. Barclay, T. G.; Hegab, H. M.; Clarke, S. R.; Ginic-Markovic, M. Versatile Surface Modification Using Polydopamine and Related Polycatecholamines: Chemistry, Structure, and Applications. *Adv. Mater. Interfaces* **2017**, *4*, 1601192.

20. Hong, S.; Na, Y. S.; Choi, S.; Song, I. T.; Kim, W. Y.; Lee, H. Non-Covalent Self-Assembly and Covalent Polymerization Co-Contribute to Polydopamine Formation. *Adv. Funct. Mater.*, **2012**, 22, 4711-4717.
21. Della Vecchia, N. F.; Avolio, R.; Alfè, M.; Errico, M. E.; Napolitano, A.; d'Ischia, M. Building-Block Diversity in Polydopamine Underpins a Multifunctional Eumelanin-Type Platform Tunable Through a Quinone Control Point. *Adv. Funct. Mater.*, **2013**, 23, 1331-1340.
22. Chen, C. T.; Ball, V.; de Almeida Gracio, J. J.; Singh, M. K.; Toniazzi, V.; Ruch, D.; Buehler, M. J. Self-assembly of tetramers of 5,6-dihydroxyindole explains the primary physical properties of eumelanin: experiment, simulation, and design. *ACS Nano*. **2013**, 7(2), 1524-1532.
23. Alfieri, M. L.; Micillo, R.; Panzella, L.; Crescenzi, O.; Oscurato, S. L.; Maddalena, P.; Napolitano, A.; Ball, V.; d'Ischia, M. Structural Basis of Polydopamine Film Formation: Probing 5,6-Dihydroxyindole-Based Eumelanin Type Units and the Porphyrin Issue. *ACS Appl. Mater. Interfaces* **2018**, 10, 7670-7680.
24. Della Vecchia, N. F.; Luchini, A.; Napolitano, A.; D'Errico, G.; Vitiello, G.; Szekely, N.; d'Ischia, M.; Paduano, L. Tris Buffer Modulates Polydopamine Growth, Aggregation, and Paramagnetic Properties. *Langmuir* **2014**, 30, 9811-9818.
25. Byun, J. B.A. Study of Polydopamine Surface Adhesion and Procedure Development of Polydopamine Film Formation via Spin Coating. Mount Holyoke College, South Hadley, MA, 2019.
26. Bernsmann, F.; Ball, V.; Addiego, F.; Ponche, A.; Michel, M.; Gracio, José Joaquin de Almeida; Toniazzi, V.; Ruch, D. Dopamine–Melanin Film Deposition Depends on the Used Oxidant and Buffer Solution. *Langmuir* **2011**, 27, 2819-2825.
27. Zhang, C.; Ou, Y.; Lei, W.; Wan, L.; Ji, J.; Xu, Z. CuSO₄/H₂O₂-Induced Rapid Deposition of Polydopamine Coatings with High Uniformity and Enhanced Stability. *Angew. Chem. Int. Ed.* **2016**, 55, 3054-3057.
28. Ponzio, F.; Barthès, J.; Bour, J.; Michel, M.; Bertani, P.; Hemmerlé, J.; d'Ischia, M.; Ball, V. Oxidant Control of Polydopamine Surface

- Chemistry in Acids: A Mechanism-Based Entry to Superhydrophilic-Superoleophobic Coatings. *Chem. Mater.* **2016**, 28, 4697-4705.
29. Wei, Q.; Zhang, F.; Li, J.; Li, B.; Zhao, C. Oxidant-induced dopamine polymerization for multifunctional coatings. *Polym. Chem.*, **2010**, 1, 1430-1433.
 30. Yeon, D. K.; Ko, S.; Jeong, S.; Hong, S.; Kang, S. M.; Cho, W. K. Oxidation-Mediated, Zwitterionic Polydopamine Coatings for Marine Antifouling Applications. *Langmuir* **2019**, 35, 1227-1234.
 31. Hong, S. H.; Hong, S.; Ryou, M.; Choi, J. W.; Kang, S. M.; Lee, H. Sprayable Ultrafast Polydopamine Surface Modifications. *Adv. Mater. Interfaces* **2016**, 3, 1500857.
 32. Schlaich, C.; Li, M.; Cheng, C.; Donskyi, I. S.; Yu, L.; Song, G.; Osorio, E.; Wei, Q.; Haag, R. Mussel-Inspired Polymer-Based Universal Spray Coating for Surface Modification: Fast Fabrication of Antibacterial and Superhydrophobic Surface Coatings. *Adv. Mater. Interfaces* **2018**, 5, 1701254.
 33. Park, J. H.; Choi, S.; Moon, H. C.; Seo, H.; Kim, J. Y.; Hong, S.; Lee, B. S.; Kang, E.; Lee, J.; Ryu, D. H.; Choi, I. S. Antimicrobial spray nanocoating of supramolecular Fe(III)-tannic acid metal-organic coordination complex: applications to shoe insoles and fruits. *Scientific Reports* **2017**, 7, 6980.
 34. Lawrence, C. J. The Mechanics of Spin Coating of Polymer Films. *Phys. Fluids*, **1988**, 31(10), 2786-2795.
 35. Bornside, D. E.; Macosko, C. W.; Scriven, L. E. On the Modeling of Spin Coating. *Journal of Imaging Technology*, **1987**, 13, 122-130.
 36. Klosterman, L.; Riley, J. K.; Bettinger, C. J. Control of Heterogeneous Nucleation and Growth Kinetics of Dopamine-Melanin by Altering Substrate Chemistry. *Langmuir* **2015**, 31, 3451-3458.
 37. Teisala, H.; Baumli, P.; Weber, S. A. L.; Vollmer, D.; Butt, H. Grafting Silicon at Room Temperature - a Transparent, Scratch-resistant Nonstick Molecular Coating. *Langmuir*, **2020**, 36, 4416-4431.
 38. Weinhold, F.; West, R. The Nature of the Silicon-Oxygen Bond. *Organometallics*, **2011**, 30, 5815-5824.

39. Chen, W. NSF Proposal 2013.